Optical birefringence and acoustic properties near the phase transitions and triple point in incommensurate proper ferroelastic Cs_2HgBr_4, Cs_2CdBr_4 and Cs_2HgCl_4 crystals

1993 J. Phys.: Condens. Matter 5 5189

(http://iopscience.iop.org/0953-8984/5/29/014)

J. Phys.: Condens. Matter 5 (1993) 5189–5200. Printed in the UK

Optical birefringence and acoustic properties near the phase transitions and triple point in incommensurate proper ferroelastic Cs_2HgBr_4, Cs_2CdBr_4 and Cs_2HgCl_4 crystals

A V Kityk, O M Mokry, V P Soprunyuk and O G Vlokh
Lviv State I Franko University, 1 Universitetska Street, 290602 Lviv, Ukraine

Received 12 January 1993, in final form 10 March 1993

Abstract. The influence of hydrostatic pressure on the temperature dependences of the optical birefringence and ultrasonic velocities is studied in the vicinity of the phase transition temperatures of Cs_2HgBr_4, Cs_2CdBr_4 and Cs_2HgCl_4 crystals. The new polycritical triple points, which separate the normal, incommensurate and proper ferroelastic phases, have been found in the P–T phase diagrams of all the compounds at applied pressures of 140 MPa, 100 MPa and 140 MPa, respectively. The origin of the triple points and the acoustic and optical properties near the phase transitions are discussed within the framework of phenomenological theory.

1. Introduction

It is well known that external influences (electric field, mechanical stress, hydrostatic pressure, etc) essentially distort the structure of the incommensurate (I) phases of ferroelectric and ferroelastic crystals. In many cases it leads to the appearance of triple points in their phase diagrams, where the two lines of the I phase transitions (PTs) merge into the one line of normal (N)-to-commensurate (C) PTs. In I proper ferroelectric crystals such points are often called the Lifshitz points (Hornreich *et al* 1975). The wavevector of the I modulation k_0 and the angle between the tangents to the lines of I PTs become close to zero in the vicinity of the Lifshitz point, which is the main peculiarity of this kind of triple point. For the first time the Lifshitz point of ferroelectric materials has been experimentally found in the (x, T) phase diagram of the solid solution compound $Sn_2P_2(S_{1-x}Se_x)_6$ (see the review article by Vysochansky and Slivka (1992)). The phenomenological theory of the Lifshitz point has been previously considered in detail by Hornreich *et al* (1975) and Michelson (1977). At the same time, one would expect some peculiarities in the triple points in the case of I proper ferroelastic (PF) crystals. This is because the appropriate variables for the homogeneous state are the components of elastic strain tensor, while for the inhomogeneous state they are the components of the displacement vector. Consequently, as has been shown by Vlokh *et al* (1989a), despite the fact that the N-to-C transition is of the second order the value of k_0 is finite at the Lifshitz point and at this point no common tangent to the lines of the I-to-PF and N-to-I PTs exists. This caused great interest in the investigation of the nature of such new polycritical phenomena using both experimental and theoretical methods.

The triple points separating the N, I and C PF phases have been found in our previous studies (Vlokh *et al* 1989c, 1990d) in the pressure–temperature (P–T) phase diagrams of Cs_2HgBr_4 and Cs_2CdBr_4 crystals by the optical birefringence method. At atmospheric

0953-8984/93/295189+12$07.50

pressure, Cs_2HgBr_4 undergoes four consecutive PTs: from the orthorhombic N phase (space group, *Pnma*) to the I phase at $T_i = 243$ K, to the monoclinic PF phase (space group, $P2_1/n11$) at $T_c = 230$ K, to the triclinic PF phase (space group, $P\bar{1}$) at $T_1 = 165$ K and, finally, to the triclinic phase (space group, $P\bar{1}$) with a doubled period of the unit cell in the *b* direction at $T_2 = 85$ K (Plesko *et al* 1980a, 1981). A similar sequence of PTs occurs in the isomorphous Cs_2CdBr_4 compound: from the N phase (space group, *Pnma*) to the I phase at $T_i = 252$ K to the monoclinic PF phase (space group, $P2_1/n11$) at $T_c = 237$ K to the triclinic PF phase (space group, $P\bar{1}$) at $T_1 = 158$ K (Plesko *et al* 1980a, Maeda *et al* 1983). The soft mode associated with the N-to-I PT in these crystals consists mainly of the rotation of the rigid XBr_4 tetrahedra (X ≡ Cd, Hg) around the *a* axis (Plesko *et al* 1980b, Nakatama *et al* 1987). The wavevector k_0 in the I phase is close to the centre of the Brillouin zone ($k_0 = \delta a^*$, where $\delta \simeq 0.15$ at $T = T_i$ and $a^* = 2\pi/a$ is the reciprocal-lattice parameter), i.e. one is dealing with an I phase of type II according to the classification of Bruce and Cowley (1978). For Cs_2HgBr_4 and Cs_2CdBr_4 the lines of the N-to-I and I-to-PF PTs merge into the line of N-to-PF PTs at hydrostatic pressures P_k of 140 MPa and 100 MPa, respectively (Vlokh *et al* 1989c, 1990d).

Cs_2HgCl_4 crystals have not been sufficiently well studied on the whole. On cooling, these crystals undergo six successive PTs at $T_i = 220$ K, $T_c = 195$ K, $T_1 = 184$ K, $T_2 = 182$ K, $T_3 = 166$ K and $T_4 = 164$ K (Kallayev *et al* 1990). The high-temperature N phase has a prototype structure of *Pnma* similar to Cs_2HgBr_4 and Cs_2CdBr_4. Between T_i and T_c the system exhibits the I phase according to the results of nuclear magnetic resonance measurements (Boguslavsky *et al* 1983). The symmetry and nature of all the other low-temperature phases are still unknown. Only dielectric (Kallyev *et al* 1990), optical and acoustic measurements (Vlokh *et al* 1990a) have been performed previously in a wide temperature range including the region of the PTs.

Acoustic and optical measurements have been widely used in the investigation of numerous I ferroelectric and ferroelastic crystals. In recent years these methods were also successfully employed in investigations of the *P–T* phase diagrams and polycritical phenomena in I crystals of the A_2BX_4 group (Vlokh *et al* 1989b,c, 1990b,c,d). In this paper we report our experimental results on the influence of the hydrostatic pressure on the temperature behaviour of the optical birefringence and acoustic properties in the vicinity of PTs and polycritical points of I Cs_2HgBr_4, Cs_2CdBr_4 and Cs_2HgCl_4 crystals. Some of these results concerning the Cs_2HgBr_4 and Cs_2CdBr_4 compounds have been published previously (Vlokh *et al* 1989c, 1990c, 1991). The *P–T* phase diagrams and acoustic and optical properties in the region of the PT points are considered in detail within the framework of phenomenological theory.

2. Experiments

Single crystals of Cs_2HgBr_4, Cs_2CdBr_4 and Cs_2HgCl_4 were grown from the melt by the Bridgman method. The crystallographic axes were determined by the x-ray diffraction method. We use the following crystallographic orientation: $c = Z > a = X > b = Y$ ($c \approx \sqrt{3}b$, where *a* is the pseudohexagonal axis). The plane-parallel specimens are typically 4 mm × 4 mm × 4 mm in size.

The temperature dependences of the optical birefringence were studied by Senarmonth's method using an He–Ne laser beam ($\lambda = 632.8$ nm) with an accuracy of up to 10^{-7}. Velocity changes of the longitudinal and shear ultrasound waves (USWs) were measured by the pulse-echo overlap method (Papadakis 1967) with an accuracy of the order of 10^{-4}–10^{-5}. The

accuracy of the absolute velocity determination was about 0.5%. The acoustic waves in the samples were excited by $LiNbO_3$ transducers (resonance frequency $f = 10$ MHz, band width $\Delta f = 0.1$ MHz and acoustic power $P_a = 1$–2 W). Optical and acoustic investigations under an applied hydrostatic pressure were performed at 0.1–200 MPa and 150–300 K using a high-pressure optical camera with a rate of temperature change of about 0.1 K min^{-1}.

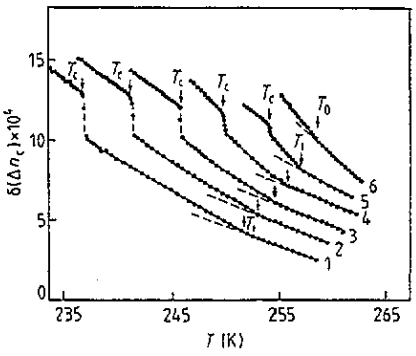

Figure 1. The temperature dependences of the optical birefringence along the c axis of Cs_2CdBr_4 crystals at different pressures P: curve 1, 0.1 MPa; curve 2, 20 MPa; curve 3, 40 MPa; curve 4, 60 MPa; curve 5, 80 MPa; curve 6, 100 MPa.

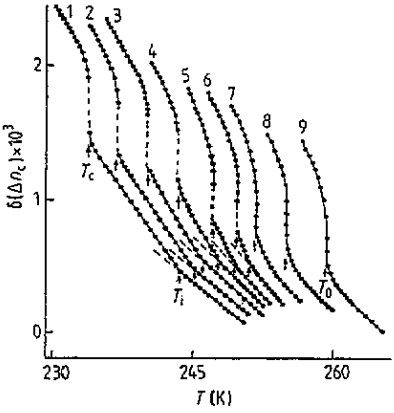

Figure 2. The temperature dependences of the optical birefringence along the c axis of Cs_2HgBr_4 crystals at different pressures P: curve 1, 0.1 MPa; curve 2, 25 MPa; curve 3, 50 MPa; curve 4, 75 MPa; curve 5, 110 MPa; curve 6, 125 MPa; curve 7, 140 MPa; curve 8, 170 MPa; curve 9, 205 MPa.

3. Experimental results

The temperature dependences of the optical birefringence along the c axis of Cs_2CdBr_4 and Cs_2HgBr_4 crystals at different values of the hydrostatic pressure P are shown in figures 1 and 2, respectively. At the normal pressure ($P = 0.1$ MPa) the temperature dependence of the birefringence changes $\delta(\Delta n_c)$ for both compounds shows a clear anomalous behaviour in the vicinity of the N-to-I ($T = T_i$) and I-to-PF ($T = T_c$) PTs. In particular, a discontinuity near T_c and a kink in the curves at T_i correspond to the first- and second-order PTs, respectively. Under applied pressure the N-to-I and I-to-PF PTs shift to the high-temperature region. At the same time the temperature width of the I phase decreases and, when the pressure P_k is higher than 140 MPa for Cs_2HgBr_4 and 100 MPa for Cs_2CdBr_4, only a single anomaly in the $\delta(\Delta n_c)$ temperature dependences occurs in the vicinity of the direct N-to-PF PT. There is good agreement between the results of optical birefringence and acoustic measurements. The latter are presented in figures 3–5. Clear kinks in the temperature dependences of the longitudinal USW velocity V_3 ($q \| c$; $E \| c$; q is the wavevector of the USW and E is its polarization) for Cs_2HgBr_4 (figure 3) and of the longitudinal USW velocity V_2 ($q \| b$; $E \| b$) for Cs_2CdBr_4 (figure 4) are observed near the N-to-I PT temperature T_i. Essentially jump-like decreases in both USW velocities V_2 and V_3 occur in the vicinity of the I-to-PF PT ($T = T_c$) for $P < P_k$ and in the vicinity of the direct N-to-PF PT ($T = T_0$) for $P > P_k$ as well. The

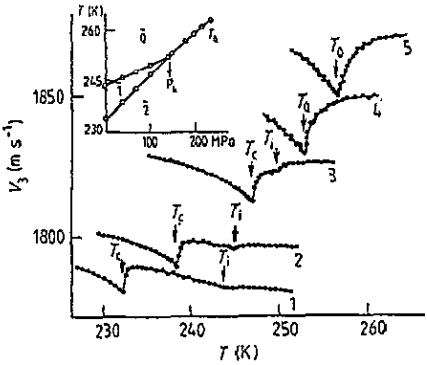

Figure 3. The temperature dependences of the longitudinal USW velocity V_3 of Cs_2HgBr_4 crystals at different pressures P: curve 1, 0.1 MPa; curve 2, 40 MPa; curve 3, 105 MPa, curve 4, 145 MPa; curve 5, 180 MPa. The inset shows the P–T phase diagram of Cs_2HgBr_4 crystals.

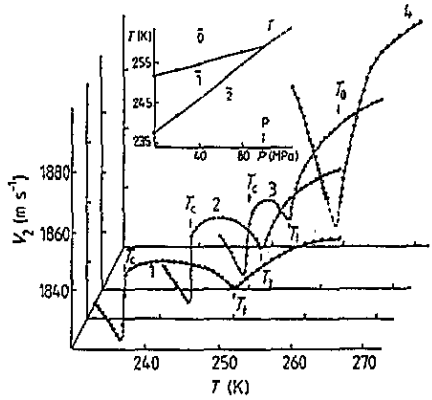

Figure 4. The temperature dependences of the longitudinal USW velocity V_2 of Cs_2CdBr_4 crystals at different pressures P: curve 1, 0.1 MPa; curve 2, 30 MPa; curve 3, 56 MPa; curve 4, 102 MPa. The inset shows the P–T phase diagram of Cs_2CdBr_4 crystals: $\tilde{0}$, N phase; $\tilde{1}$, I phase; $\tilde{2}$, PF phase.

P–T phase diagrams obtained from the acoustic and optical measurements are presented for both compounds in the insets of figures 3 and 4.

Figure 5 shows the temperature dependences of the shear USW velocity V_4 ($\boldsymbol{q}\|c$; $\boldsymbol{E}\|b$) at different pressures for Cs_2CdBr_4 crystals. On decrease in the temperature the velocity of this USW in the I phase firstly increases and then essentially decreases. Clear thermal hysteresis is observed here on heating and cooling, which is a main feature of the I phases. The nature of this effect has been considered in our previous work (Vlokh *et al* 1990c). A discontinuity in V_4 occurs in the region of the I-to-C PT. The temperature changes in V_4 for the N and I phases become sharper under an applied hydrostatic pressure. The latter is very clearly observed at a pressure close to P_k, where an anomalous decrease in V_4 occurs in the region of the PT temperatures T_i ($P < P_k$) and T_0 ($P > P_k$). Similar softening of the relevant elastic constant C_{44} is observed for isomorphous Cs_2HgBr_4 (Vlokh *et al* 1991), but in this case such softening takes place in a very narrow temperature region (1 K) near T_0. Strong USW attenuation complicates the acoustic investigation in the vicinity of the N-to-PF PT.

At atmospheric pressure the temperature dependence of the optical birefringence of Cs_2HgCl_4 crystals (figure 6) near the N-to-I PT is quite similar to the corresponding dependences for Cs_2HgBr_4 and Cs_2CdBr_4 compounds. The PT from phase $\tilde{2}$ to phase $\tilde{3}$ ($T = T_1$) is accompanied by a jump-like increase in optical birefringence. On increase in pressure the PT line $T_1(P)$ splits at $P \simeq 12$ MPa into two PT lines $T_L(P)$ and $T_l(P)$ with the appearance of a new phase $\tilde{4}$ (see figure 8, inset). The PTs into this phase are clearly manifested in the jump-like changes in the optical birefringence (figure 6) and both longitudinal V_2 ($\boldsymbol{q}\|b$; $\boldsymbol{E}\|b$) (figure 7) and shear V_4 ($\boldsymbol{q}\|c$; $\boldsymbol{E}\|b$) (figure 8) and V_5 ($\boldsymbol{q}\|c$; $\boldsymbol{E}\|a$) (figure 9) USW velocities. Under an applied hydrostatic pressure the temperature width of the I phase and phase $\tilde{2}$ (according to Kallayev *et al* (1990) this phase is probably of an improper ferroelectric type) decreases and finally these phases disappear in the triple points at $P > P_k = 140$ MPa and $P > P_k = 90$ MPa, respectively (figure 8, inset). It is necessary to mention that the temperature changes in shear USW velocity V_4 in the N and I phases become essentially sharper near T_i as the pressure increases. The anomalous decrease in

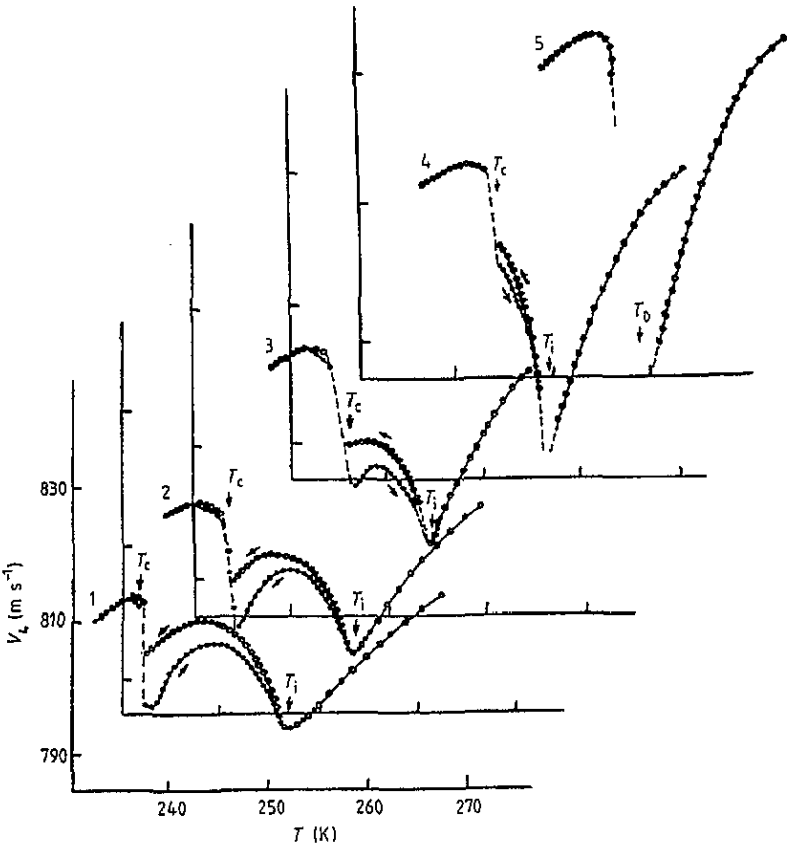

Figure 5. The temperature dependences of the shear USW velocity V_4 of Cs_2CdBr_4 crystals at different pressures P on heating (●) and on cooling (○): curve 1, 0.1 MPa; curve 2, 20 MPa; curve 3, 40 MPa; curve 4, 74 MPa; curve 5, 102 MPa.

V_4 occurs in the vicinity of the direct PT from the N phase to phase $\tilde{4}$ at $T = T_0$ ($P > P_k$) quite similarly to those in Cs_2HgBr_4 and Cs_2CdBr_4 (figure 5) compounds. Together with the domain structure, which is observed in polarized light in the a cut of crystals in phase $\tilde{4}$, the latter indicates that the pressure-induced phase $\tilde{4}$ of Cs_2HgCl_4 crystals is obviously of the PF type.

4. Discussion

4.1. P–T phase diagram

The phenomenological theory of the P–T phase diagram for the I PF crystal of Cs_2HgBr_4 type has been considered in detail in our previous work (Vlokh *et al* 1989a). Here we present the main results of such considerations in comparison with the experimental data.

For the case concerning the N-to-PF PT the order parameter transformation properties are equivalent to those of the strain tensor U_{yz}. On the contrary the wavevector of the I phase is parallel to the $X(a)$ axis, i.e. inhomogeneous strains may correspond to the U_{ik} components containing no other components but X derivatives only. It is obvious that no inhomogeneous

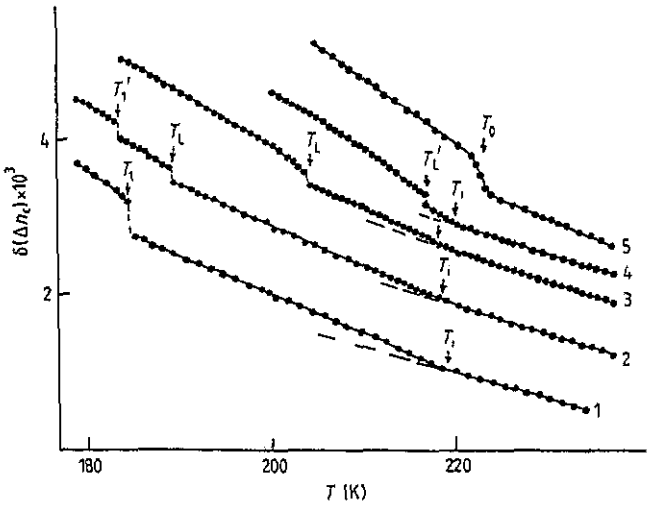

Figure 6. The temperature dependences of the optical birefringence along the c axis of Cs_2HgCl_4 crystals at different pressures P: curve 1, 0.1 MPa; curve 2, 27 MPa; curve 3, 76 MPa; curve 4, 127 MPa; curve 5, 156 MPa.

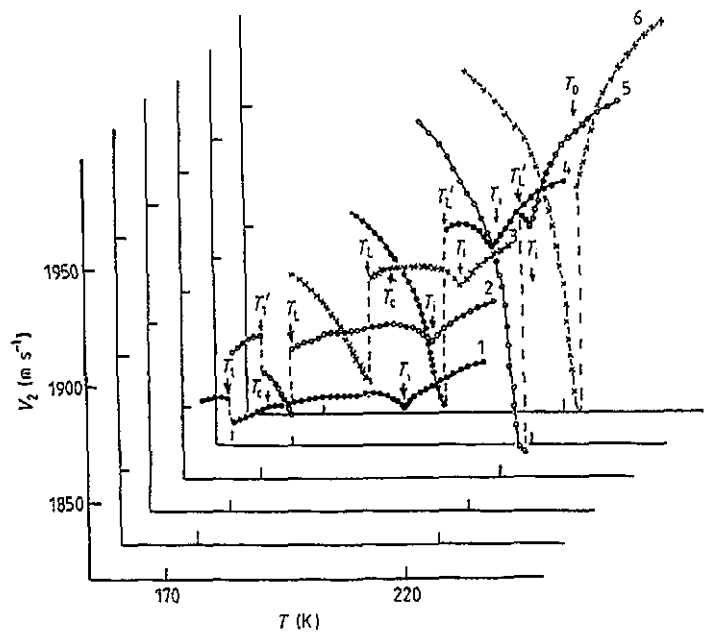

Figure 7. The temperature dependences of the longitudinal USW velocity V_2 of Cs_2HgCl_4 crystals at different pressures P: curve 1, 0.1 MPa; curve 2, 27 MPa; curve 3, 59 MPa; curve 4, 88 MPa; curve 5, 127 MPa; curve 6, 157 MPa.

strain corresponding to the U_{yz} component would appear in that case. Considering hence the PT into the I phase a certain optical coordinate Q with the U_{yz} transformation properties should be used as the order parameter. As has been pointed out above, the physical meaning of Q is the rotation of the MX_4 (M ≡ Hg, Cd; X ≡ Cl, Br) tetrahedra around the X axis.

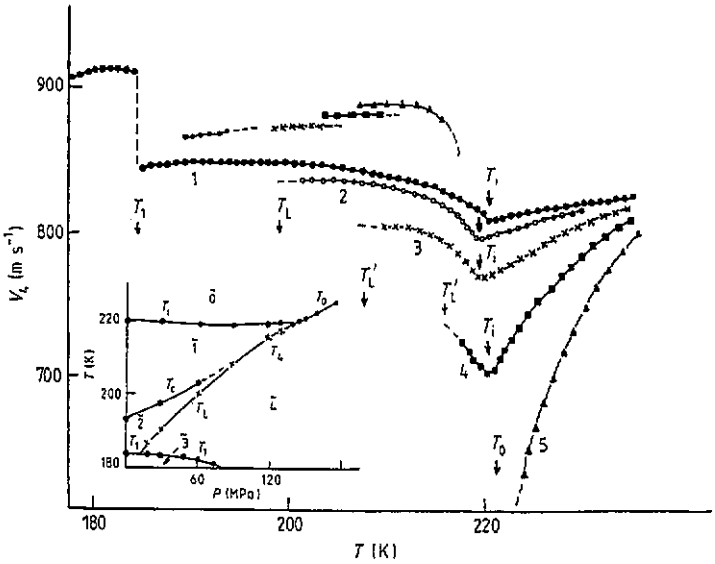

Figure 8. The temperature dependences of the shear USW velocity V_4 of Cs_2HgCl_4 crystals at different pressures P: curve 1, 0.1 MPa; curve 2, 57 MPa; curve 3, 86 MPa; curve 4, 118 MPa; curve 5, 147 MPa. The inset shows the P–T phase diagram of Cs_2HgCl_4 crystals: $\tilde{0}$, N phase; $\tilde{1}$, I phase; $\tilde{2}$, improper ferroelectric phase; $\tilde{3}$, improper ferroelastic phase; $\tilde{4}$, monoclinic PF phase.

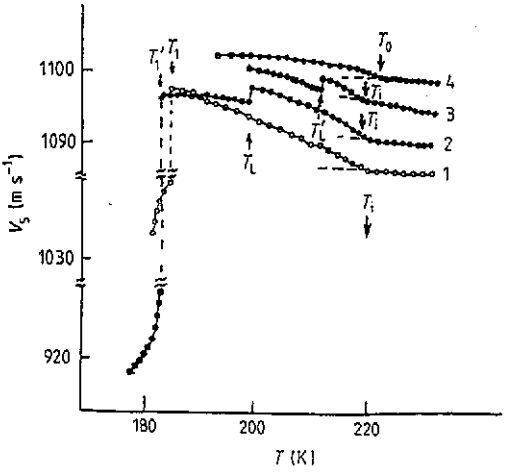

Figure 9. The temperature dependences of the shear USW velocity V_5 of Cs_2HgCl_4 crystals at different pressures P: curve 1, 0.1 MPa; curve 2, 56 MPa; curve 3, 108 MPa; curve 4, 157 MPa.

We use the thermodynamic Landau potential density in the form

$$\tilde{F} = \tfrac{1}{2}AQ^2 + \tfrac{1}{2}g(\partial Q/\partial x)^2 + \tfrac{1}{2}h(\partial^2 Q/\partial x^2)^2 + \tfrac{1}{4}BQ^4 + \alpha Q U_{yz} + \epsilon U_{yz}^2 \tag{1}$$

where as usual $A = A_0(T - \Theta)$ and $A_0, B, h, \alpha > 0$. After the minimization with respect to homogeneous strains, one can obtain the following expression:

$$F = \int \tilde{F}\,\mathrm{d}x = \left(\tfrac{1}{2}A - \frac{\alpha^2}{2\epsilon}\right) Q_0^2 + \tfrac{1}{2}\sum_{k\neq 0}(A + gk^2 + hk^4) Q_k Q_{-k}$$
$$+ \tfrac{1}{4}B \sum_{k_1 k_2 k_3 k_4} Q_{k_1} Q_{k_2} Q_{k_3} Q_{k_4} \delta(k_1 + \ldots + k_4). \tag{2}$$

As follows from equation (2), the N-to-I ($A_i = A_0(T_i - \Theta)$), I-to-PF ($A_c = A_0(T_c - \Theta)$) and N-to-PF ($A_* = A_0(T_0 - \Theta)$) PT lines in the (A, g) phase plane are determined by the conditions

$$A_i = g^2/4h \qquad A_c = (\sqrt{6}+2)(\alpha^2\sqrt{6}/2\epsilon - g^2/4h) \qquad A_* = \alpha^2/\epsilon \quad (3)$$

and the equilibrium value of the I modulation vector $k_0 = \sqrt{-g/2h}$. It is easy to see that the PT lines merge at the triple point of the (A, g) phase plane, if $g = g_k = -2\alpha\sqrt{h/\epsilon} < 0$ (figure 10). Consequently the wavevector of the I modulation k_0 and the angle γ between the tangents to the lines of N-to-I and I-to-C PTs have finite values at the triple point:

$$k^* = (\alpha\sqrt{1/\epsilon h})^{1/2} \quad (4)$$

$$\gamma = \tan^{-1}\{\alpha\sqrt{1/h\epsilon}(\sqrt{6}+3)/[1-(\alpha^2/h\epsilon)(\sqrt{6}+2)]\}. \quad (5)$$

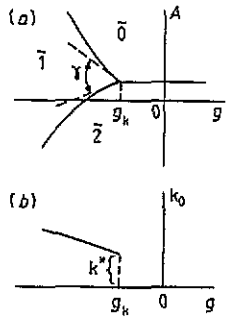

Figure 10. (*a*) Phase diagram in the (A, g) phase plane and (*b*) the dependence of the wavevector k_0 on the coefficient g in the region of the triple point.

The latter is a characteristic feature of this kind of I ferroelastic crystal and essentially distinguishes them from I proper ferroelectrics. Returning to the experimental results it is necessary to pay attention to two peculiarities of the P–T phase diagrams for the Cs_2XY_4 group crystals. The first is that the temperature width of the I phase does not depend quadratically on the applied hydrostatic pressure in contrast with the case for I proper ferroelectric crystals (Vysochansky and Slivka 1992). The second peculiarity is that no common tangent to the N-to-I and I-to-PF PT lines exists at the triple point. It is easy to see (figures 3, 4 and 8 insets) that these lines merge at the triple point for a finite value of the angle. Consequently we may conclude that there is good qualitative agreement between the phenomenological theory and experimental data.

4.2. Optical birefringence and USW velocities

The explanation of the anomalous temperature dependences of the optical birefringence at the N-to-I PT is straightforward. This problem has been discussed previously in numerous studies (see, e.g., Konac (1979) and Vlokh *et al* (1984)). Following the phenomenological Landau theory, the anomalous changes in the optical birefringence below T_i are proportional to the square of the order parameter amplitude $|Q_{k_0}|$:

$$\delta(\Delta n_c) \sim |Q_{k_0}|^2 \sim (T_i - T)^{2\beta} \quad (6)$$

where β is the critical exponent. There is good agreement between equation (6) and the experimental results (figures 1, 2 and 6). A clear kink in the $\delta(\Delta n_c)$ temperature

dependences near the N-to-I PT appears as a result of the additional contribution of the order parameter to the optical birefringence below T_i. The temperature changes in the optical birefringence in the high-pressure region near the PT temperature T_0 may be explained in a similar way when we replace Q_{k_0} by Q_0 in equation (6), where Q_0 is the order parameter of the PF phase. The continuous changes in the optical birefringence in the vicinity of the N-to-PF PT indicate that this PT is of second order for all compounds.

Let us discuss the temperature changes in the USW velocity near the PTs and triple points. The real acoustic behaviour can be easily reproduced for the Cs_2XY_4 group of crystals by the previous phenomenological model (Rehwald *et al* 1980, Lemanov and Esayan 1987). Obviously this model can be directly employed for any I system, where the acoustic waves are coupled with the modulation structure through third- or higher-order anharmonic effects. In the case of Cs_2XY_4 crystals we use the elastic part of the free energy with the next coupling term, which corresponds to anharmonic interactions between strains U_1–U_6 and order parameter:

$$F_{Q,U} = \sum_{i=1}^{3} a_i Q_{k_0} Q_{-k_0} U_i + \tfrac{1}{2} \sum_{i=1}^{6} b_i Q_{k_0} Q_{-k_0} U_i^2 + \sum_{i=1}^{3} a_i' Q_0^2 U_i$$
$$+ \tfrac{1}{2} \sum_{i=1}^{6} b_i' Q_0^2 U_i^2 + \alpha Q_0 U_4 + f Q_{k_0}^2 Q_{2k_0}^* U_4$$

where Q_0 and Q_{k_0} are the normal phonon coordinates in the PF and I phases, respectively, and Q_{2k_0} is the normal phonon coordinate of the second-harmonic modulation, which appears under the action of USWs. Using the normal mode coordinates of the soft-mode: amplitudon and phason (Dvorak and Petzelt 1978), it is possible to express the changes in the USW velocities in the I phase (see, e.g., Rehwald *et al* (1980) and Lemanov and Esayan (1987)) as

$$\Delta V_i = (1/2\rho V_i)[b_i |Q_{k_0}|^2 - 2a_i^2 |Q_{k_0}|^2 / \omega_A^2 (1 + \Omega^2 \tau_A^2)] \qquad i = 1\text{–}3 \qquad (7)$$

$$\Delta V_4 = (1/2\rho V_4)[b_4 |Q_{k_0}|^2 - f^2 |Q_{k_0}|^4 / \omega_\varphi^2 (1 + \Omega^2 \tau_\varphi^2) - \alpha^2 / A_0 (T - \Theta)] \qquad (8)$$

$$\Delta V_5 = (1/2\rho V_5) b_5 |Q_{k_0}|^2 \qquad (9)$$

$$\Delta V_6 = (1/2\rho V_6) b_6 |Q_{k_0}|^2 \qquad (10)$$

where $\Omega = qV$ is the USW frequency, $|Q_{k_0}|^2 = (A_0/2B)(T_i - T)$ is the equilibrium value of the order parameter amplitude, ρ is the crystal density, $\omega_A^2 = 2A_0(T_i - T) + hq^2$ and τ_A are the amplitudon frequency and relaxation time, respectively, and $\omega_\varphi^2 = h(a^*\delta)^2$ and τ_φ are the non-Goldstone phason frequency and relaxation time, respectively. In equation (8), only the non-Goldstone phason contribution is considered, since $\omega_A \gg \omega_\varphi$ far from T_i.

It follows from (7) that the value of the longitudinal USW velocities V_1–V_3 should exhibit a jump-like decrease at $T = T_i$, which is caused by the interaction between USWs and amplitudons. Moreover, equation (7) does not lead to any effect above T_i, contrary to experimental evidence, indicating a gradual decrease in all the longitudinal USW velocities in the N phase near T_i. Obviously, the origin of such behaviour is connected with fluctuation effects. A detailed description of the fluctuation contributions to the acoustic properties near the N-to-I PT has been given by Li *et al* (1990) in the framework of the fluctuation integral

theory. According to such considerations the additional fluctuation contribution ΔV_i^{fl} to the changes in the longitudinal USW velocities may be written as

$$\Delta V_i^{\mathrm{fl}} = -\frac{1}{2\rho V_i}\frac{16k_{\mathrm{B}}T}{(2\pi)^3}a_i^2\int\frac{\mathrm{d}^3k}{\omega_0^4(k)[4+\Omega^2\tau_0^2(k)]} \qquad T > T_{\mathrm{i}} \tag{11a}$$

$$\Delta V_i^{\mathrm{fl}} = -\frac{1}{2\rho V_i}\frac{8k_{\mathrm{B}}T}{(2\pi)^3}a_i^2\left(\int\frac{\mathrm{d}^3k}{\omega_{\mathrm{A}}^4(k)[4+\Omega^2\tau_{\mathrm{A}}^2(k)]}+\int\frac{\mathrm{d}^3k}{\omega_\varphi^4(k)[4+\Omega^2\tau_\varphi^2(k)]}\right) \qquad T < T_{\mathrm{i}} \tag{11b}$$

where $\omega_0(k)$ is the soft-mode dispersion curve in the N phase, $\omega_{\mathrm{A}}(k)$ and $\omega_\varphi(k)$ are the dispersion curves of amplitudon and phason frequencies, respectively, in the I phase and $\tau_0(k)$, $\tau_{\mathrm{A}}(k)$ and $\tau_\varphi(k)$ are the corresponding relaxation times. Note that in equations (11*a*) and (11*b*) the main contribution to the fluctuation integrals comes from the vicinities of the regions in the Brillouin zone where $\omega_0(k)$, $\omega_{\mathrm{A}}(k)$ and $\omega_\varphi(k)$ have minima. In the case of the direct PT from the N to the PF phase at $P \gg P_{\mathrm{k}}$, which is equivalent to $g > 0$ in the (A, g) phase plane (figure 10), the soft-mode dispersion $\omega_0^2 = A_0(T-\Theta)+gk^2+hk^4$ shows a clear minimum in the Brillouin zone centre. Consequently the main contribution to the integral comes only from the narrow vicinity of $k = 0$. Quite a different situation takes place in the case when the coefficient g becomes negative and two minima occur in the soft-mode dispersion at $k_\pm = \pm\sqrt{-g/2h}$. The soft-mode frequency is low at $T \to T_{\mathrm{i}}$ in a relatively wider region of k, between k_+ and k_-. As a result of this, the fluctuation integrals (11*a*) and (11*b*) considerably increase, leading to a clear anomalous decrease in the USW velocities V_1–V_3 in the N and I phases near T_{i}. Obviously, fluctuation effects should also be clearly observed in the vicinity of T_0 not far from the triple point.

Besides that, the Landau–Khalatnikov mechanism is manifest in the real behaviour of the longitudinal USW velocities directly at $T = T_0$ ($P \gg P_{\mathrm{k}}$) (figures 3, 4 and 7). The second term in equation (7) adequately describes this contribution if we consider that $Q_{k_0} \to Q_0$, $a_i \to a_i'$, $\omega_{\mathrm{A}} \to \omega_0$ and $\tau_{\mathrm{A}} \to \tau_0$. Returning to the experimental results it should be noted that they are in good qualitative agreement with the phenomenological treatment. Unfortunately numerical calculations have not been carried out since experimental data concerning the soft-mode dispersion in the Cs_2XY_4 group of crystals are not available.

Let us consider the behaviour of the shear USW velocities in the region of PTs. Near the N-to-I PT the variation in $\Delta V_4(T)$ (figures 5 and 8) and $\Delta V_5(T)$ (figure 9) can be explained by the first term in equation (8) and the first term in equation (9), respectively, considering the fourth-order anharmonicity $b_i Q_{k_0} Q_{-k_0} U_i^2$ coupling. In these cases the $V_i(T)$ temperature dependences show kinks at $T = T_{\mathrm{i}}$ and the additional velocity changes below T_{i} are proportional to the square of the order parameter amplitude. The observed decrease in V_4 with decreasing temperature is caused by the second and third terms in equation (8). In particular this is due to the faster increase in $|Q_{k_0}|^4/\omega_\varphi^2$ (at $\delta \to 0$, $\omega_\varphi = h(a^*\delta)^2 \to 0$) in comparison with $|Q_{k_0}|^2$. Thus, contrary to the I proper ferroelectric crystals (Lemanov and Esayan 1987), the non-Goldstone phason contribution clearly manifests itself in I PF crystals. Typical changes in the V_4 temperature dependences at high pressures are caused by the considerable increase in the role of the $\alpha Q_0 U_4$ coupling term. Elastic softening is clearly seen in the region of the direct PT from the N to the PF phase at $P > P_{\mathrm{k}}$, where the changes in V_4 are described by a Curie–Weiss law:

$$\Delta V_4 = -(1/2\rho V_4)[\alpha^2/A_0(T-T_0)] \qquad T > T_0 \tag{12a}$$

$$\Delta V_4 = -(1/2\rho V_4)[\alpha^2/2A_0(T-T_0)] \qquad T < T_0 \tag{12b}$$

where, according to equation (3), $T_0 = \Theta + \alpha^2/A_0\epsilon$. The temperature dependences of V_4 observed near T_0 (figures 5 and 8) suggest the existence of the N-to-PF PT.

5. Conclusion

We have investigated the influence of the hydrostatic pressure on the temperature behaviour of optical birefringence and USW velocities in Cs_2XY_4 (X ≡ Cd, Hg; Y ≡ Cl, Br) compounds. Triple points separating the N, I and PF phases have been found in their P–T phase diagrams. The P–T phase diagrams obtained are considered within the framework of the phenomenological Landau theory. The main result of this consideration is that the triple point in the I PF compounds of Cs_2HgCl_4 type essentially differs from the Lifshitz triple point in the P–T phase diagram of the I proper ferroelectric compounds. In particular, the wavevector of the I modulation and angle between the tangents to the lines of the N-to-IC and IC-to-C PTs have finite values at the triple point. There is fairly good qualitative agreement between phenomenological theory considerations and experimentally obtained P–T diagrams for all compounds of the Cs_2XY_4 group.

Explanations of the acoustic properties near the phase transition and triple points are given in the framework of the frequently used previous phenomenological model (Rehwald *et al* 1980, Lemanov and Esayan 1987). Moreover, the real acoustic behaviour near N-to-I and N-to-PF PTs can be correctly described if fluctuation effects are taken into account. The latter are considered on the basis of the fluctuation integral theory (Li *et al* 1990). Although numerical calculations have not been carried out, since data on soft-mode dispersion in Cs_2XY_4 are not available, there is good qualitative agreement between experiments and the theoretical treatment. Naturally, a more unambiguous phenomenological analysis may be performed in the future, when the necessary inelastic neutron diffraction data have been obtained. Elastic softening has been found in the V_4 temperature dependences at high pressures, where the direct PT from the N to the PF phase occurs. The change in V_4 at $P \geqslant P_k$ is well described by a Curie–Weiss law, suggesting thus the existence of the direct PT from the N to the PF phase.

Acknowledgments

This work was supported by the Ukraine State Committee of Science and Technology (under the programme 'Optical properties of ferric crystals near the phase transitions').

References

Bogusiavsky A A, Lotfullyn R Sh and Simonov M V 1983 *Fiz. Tverd. Tela* **27** 523
Bruce A D and Cowley R A 1978 *J. Phys. C: Solid State Phys.* **11** 3609
Dvorak V and Petzelt J 1978 *J. Phys. C: Solid State Phys.* **11** 4827
Hornreich R M, Luban M and Strikman S 1975 *Phys. Rev. Lett.* **35** 1678
Kallayev S N, Gladkii V V, Kirikov V A and Kamilov I K 1990 *Ferroelectrics* **106** 299
Konac C 1979 *Phys. Status Solidi* a **54** 99
Lemanov V V and Esayan S Kh 1987 *Ferroelectrics* **73** 125
Li G, Tao N, Hong L V, Cummins H Z, Dreyfus C, Hebbache M, Pick R M and Vagner J 1990 *Phys. Rev.* B **42** 4406
Maeda M, Honda A and Yamada N 1983 *J. Phys. Soc. Japan* **52** 3219
Michelson A 1977 *Phys. Rev.* B **16** 577

Nakatama H, Nakatama N and Chihara H 1987 *J. Phys. Soc. Japan* **56** 2927
Papadakis E P 1967 *J. Acoust. Soc. Am.* **42** 1045
Plesko S, Dvorak V, Kind R and Treindl H 1981 *Ferroelectrics* **36** 331
Plesko S, Kind R and Arend H 1980a *Phys. Status Solidi* a **61** 87
—— 1980b *Ferroelectrics* **26** 703
Rehwald W, Vonlanthen A, Kruger J K, Wallerius R and Unruh H-G 1980 *J. Phys. C: Solid State Phys.* **13** 3823
Vlokh O G, Gribik V G, Kityk A V, Mokry O M, Olekseyuk I D and Piroga S A 1990a *Kristallografiya* **35** 1483
Vlokh O G, Kaminskaya E P, Kityk A V, Levanyuk A P and Mokry O M 1989a *Sov. Phys.–Solid State* **31** 1629
Vlokh O G, Kityk A V and Mokry O M 1990b *Kristallografiya* **35** 894
Vlokh O G, Kityk A V, Mokry O M and Gribik V G 1989b *Phys. Status Solidi* a **116** 287
—— 1990c *Fiz. Tverd. Tela* **32** 1556
Vlokh O G, Kityk A V, Mokry O M and Kamínsky B V 1990d *Sov. Phys.–Crystallogr.* **35** 138
Vlokh O G, Kityk A V, Mokry O M, Kirilenko V V, Olekseyuk I D and Piroga S A 1989c *Sov. Phys.–Solid State* **31** 901
—— 1991 *Izv. Akad. Nauk SSSR, Neorg. Mater.* **27** 1740
Vlokh O G, Kityk A V and Polovinko I I 1984 *Sov. Phys.–Crystallogr.* **29** 703
Vysochansky Yu M and Slivka V Yu 1992 *Usp. Fiz. Nauk* **162** 163